differentiation and epidermal permeability barrier homoeostasis (17). The exocytosis of lamellar bodies is strongly associated with the calcium gradient (18), and a pH gradient is maintained by normal lamellar body secretion (19,20). Thus, we think the electrical potential and the calcium gradient can be seen as two sides of the same coin, and both might play key roles in various homoeostatic processes in the epidermis.

Acknowledgements

This work was funded by Shiseido Co. Ltd. JK, MG, MD performed the research. MD designed the study. SD, MN, YT, KT and YS contributed key reagents and tools. YT advised for two-photon microscopic observation. MD wrote the paper.

Conflict of interests

The authors report no conflict of interest.

References

1 Denda M, Kumazawa N. J Invest Dermatol 2002: **118**: 65–72.
2 Denda M, Ashida Y, Inoue K *et al.* Biochem Biophys Res Commun 2001: **284**: 112–117.
3 Kawai E, Nakanishi J, Kumazawa N *et al.* Exp Dermatol 2008: **17**: 688–692.
4 Denda M, Fuziwara S, Inoue K. J Invest Dermatol 2003: **121**: 362–367.
5 Träuble H, Eibl H. Proc Natl Acad Sci USA 1974: **71**: 214–219.
6 Lee S H, Choi E H, Feingold K R *et al.* J Invest Dermatol 1998: **111**: 39–43.
7 Frick M, Bertocchi C, Jennings P *et al.* Am J Physiol Lung Cell Mol Physiol 2004: **286**: L210–L220.
8 Miklavc P, Frick M, Wittekindt O H *et al.* PLoS One 2010: **5**: e10982.
9 Chattopadhyay S, Sun P, Wang P *et al.* J Biol Chem 2003: **278**: 39675–39683.
10 Ma A S, Ozers L J. Arch Dermatol Res 1996: **288**: 596–603.
11 Denda M, Nakatani M, Ikeyama K *et al.* Exp Dermatol 2007: **16**: 157–161.
12 Denda M, Tsutsumi M, Denda S. Exp Dermatol 2010: **19**: 791–795.
13 Denda M, Sokabe T, Tominaga T *et al.* J Invest Dermatol 2007: **127**: 654–659.
14 Denda M, Tsutsumi M, Goto M *et al.* J Invest Dermatol 2010: **130**: 1942–1945.
15 Reiss K, Meyer-Hoffert U, Fischer J *et al.* Exp Dermatol 2011: **20**: 905–910.
16 Denda M, Kitamura K, Elias P M *et al.* J Invest Dermatol 1997: **109**: 84–90.
17 Elias P M, Ahn S K, Denda M *et al.* J Invest Dermatol 2002: **119**: 1128–1136.
18 Menon G K, Price L F, Bommannan B *et al.* J Invest Dermatol 1994: **102**: 789–795.
19 Behne M J, Barry N P, Hanson K M *et al.* J Invest Dermatol 2003: **120**: 998–1006.
20 Tarutani M, Nakajima K, Uchida Y *et al.* J Invest Dermatol 2012: **132**: 2019–2025.

Supporting Information

Additional Supporting Information may be found in the online version of this article:

Data S1. Materials and methods.

Data S2. Two-photon microscopic observation.

Figure S1. Two-photon laser microscopic observation of lipids in human skin tissue loaded or not loaded with negative external electric potential. a: Control skin (Bar = 10 μm), b: Treated skin (Bar = 10 μm). c–g: Sections of control skin at intervals of 1 μm (Bars = 2 μm). h–l: Sections of treated skin at intervals of 1 μm (Bars = 2 μm). Longer intercellular lipid domains were observed in treated skin than in control skin. m: Three-dimensional image of treated skin. Clear intercellular lipid domains can be seen (arrows). The length of each axis is indicated.

DOI: 10.1111/exd.12149
www.wileyonlinelibrary.com/journal/EXD

Letter to the Editor

Postnatal regulation of X,K-ATPases in rat skin and conserved lateroapical polarization of Na,K-ATPase in vertebrate epidermis

Nikolay B. Pestov[1,2], Tatyana V. Korneenko[1], Mikhail I. Shakhparonov[1] and Nikolai N. Modyanov[2]

[1]Shemyakin and Ovchinnikov Institute of Bioorganic Chemistry, Russian Academy of Sciences, Moscow, Russia; [2]Department of Physiology and Pharmacology, University of Toledo College of Medicine, Toledo, OH, USA

Correspondence: Nikolay B. Pestov, PhD, Shemyakin-Ovchinnikov Institute of Bioorganic Chemistry, Miklukho-Maklaya 16/10, 117997 Moscow, Russia, Tel.:/Fax: +74953306556, e-mail: korn@mail.ibch.ru

Abstract: Development of epidermis creates stratified epithelium with different sets of ion-transporting enzymes in its layers. We have characterized expression of Na,K- and H,K-ATPase α and β subunits and FXYD isoforms in rat skin. Maturation of rat skin from newborn to adult is associated with an increase in FXYD4 and a decrease of Na,K-ATPase α1-isoform, ATP1B4 and FXYD6 transcripts. Na,K-ATPase of rat epidermis is represented predominantly by α1 and β3 isoforms. Keratinization is associated with the loss of the Na,K-ATPase α-subunit and an enrichment of αng. Na,K-ATPase α1 is abundant in the innermost layer, *stratum basale*, where it is lacking in basal membranes, thus indicating lateroapical polarization of Na,K-ATPase. Immunocytochemical detection of Na,K-ATPase in *Xenopus laevis* skin shows that cellular and subcellular localization of the enzyme has a pattern highly similar to that of mammals: basolateral in glandular epithelium and lateroapical in epidermis.

Key words: ATP12A – epidermis – P-ATPases – X, K-ATPases

Accepted for publication 3 April 2013

Background

The molecular basis of epidermal ion transport is medically relevant: mutations of Ca-ATPases SERCA2 and SPCA1 are associated with Darier (1) and Hailey–Hailey (2) diseases, respectively. Human non-gastric H,K-ATPase (first cloned from skin (3)) may also be involved in pathological processes, for example, its expression level is upregulated in epidermolysis bullosa simplex (4) and in psoriatic lesions (5).

X,K-ATPases are integral membrane proteins of the P-type ATPase class that perform inward K^+ transport using as counter ions either Na^+ (Na,K-ATPase) or H^+ (gastric and non-gastric

H,K-ATPase). In mammals, six genes are known for the catalytic X,K-ATPase α-subunit (Na,K-ATPase α1,α2,α3, α4, αg – gastric H,K-ATPase and αng – non-gastric H,K-ATPase α-subunits), five genes for the β-subunit (Na,K-ATPase β1,β2,β3, βg – gastric H,K-ATPase β-subunit, and muscle-specific βm) and seven genes encoding regulatory FXYD proteins (6). Historically, active ion transport by Na,K-ATPase was discovered in amphibian skin (7).

It has been established that acidification of the *stratum corneum* is under control of NHE1 Na/H exchanger (8). As NHE1 must work in concert with an active, energy-consuming transporter, we hypothesize that a Na,K-ATPase is important for the coupling. We also propose that the non-gastric H,K-ATPase may contribute by direct proton transfer out of the keratinocytes similarly to that in rodent anterior prostate epithelium (9).

Questions addressed

As a first step towards elucidating how the NHE exchanger is coupled to an active transporter, such as Na,K-ATPase, we have performed immunohistochemical detection of catalytic X,K-ATPase subunits in human, rat and Xenopus skin. Also, we asked which accessory subunit isoforms are expressed in the skin and which are affected by its maturation postpartum.

Experimental design

A detailed description is available in the Supplement. Briefly, expression of X,K-ATPase α and β subunit and FXYD genes was characterized by RT-PCR using whole rat skin as well as separated epidermis. For QRT-PCR, PPIA was used as a reference gene as it is stably expressed in keratinocytes (10). For immunochemistry, experimental procedures were similar to those described previously (11,12).

Results

Figure 1 illustrates detection of all known isoforms of both α and β subunits as well as six isoforms of FXYDs at the mRNA level using RT-PCR. Among α-subunits of Na,K-ATPases, only α1 is expressed abundantly in newborn epidermis. No signal was observed with primers specific for either α3 or α4, nor for the gastric H-K-ATPase α-subunit. mRNA of the non-gastric H,K-ATPase is present in both newborn and adult skin. The alternative transcript of this ATPase (referred to as variant B (13)) was not detected. Newborn epidermis contains β3 and, at low levels, β1 and βm, whereas β2 is absent from the epidermis. It is important that β3 is significantly enriched in epidermis versus whole skin, and this makes it unique among all transcripts tested in this study. No FXYD transcripts are expressed in rat skin at levels higher than in control tissues, and none is enriched

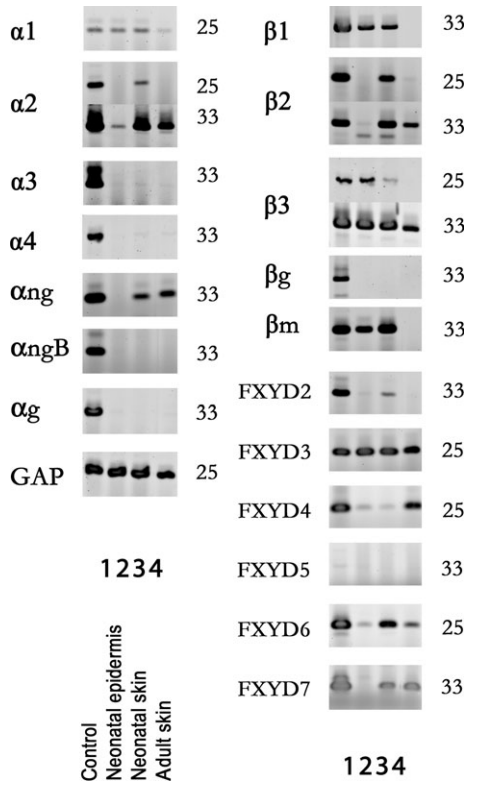

Figure 1. RT-PCR analysis of expression of X-K-ATPase α,β-subunits and FXYD proteins in rat skin. 1 – control; 2 – newborn rat epidermis; 3 – newborn rat whole skin; 4 – adult rat skin. No. of cycles used are indicated on the *right*; 33 cycles were used where high sensitivity detection was necessary. α1, α2, α3, α4, β1, β2, β3 – amplification products of mRNAs of Na-K-ATPase α1-, α2-, α3-, α4-, β1-, β2-, β3-isoforms, respectively; αg, βg and βm – gastric H,K-ATPase α-subunit and β-subunit mRNAs and muscular X,K-ATPase β-subunit, respectively; αng, αngB – non-gastric H,K-ATPase α-subunit 'canonic' and alternative mRNAs, respectively; FXYD2-6 – FXYD mRNAs; control, adult rat cDNAs from following tissues: brain for α1, α2, α3, β1, β2, β3, FXYD3, 4, 6, 7, and GAP, kidney for FXYD2, testes for α4, distal colon for αng, lung cDNA for FXYD5, stomach for αg and βg.

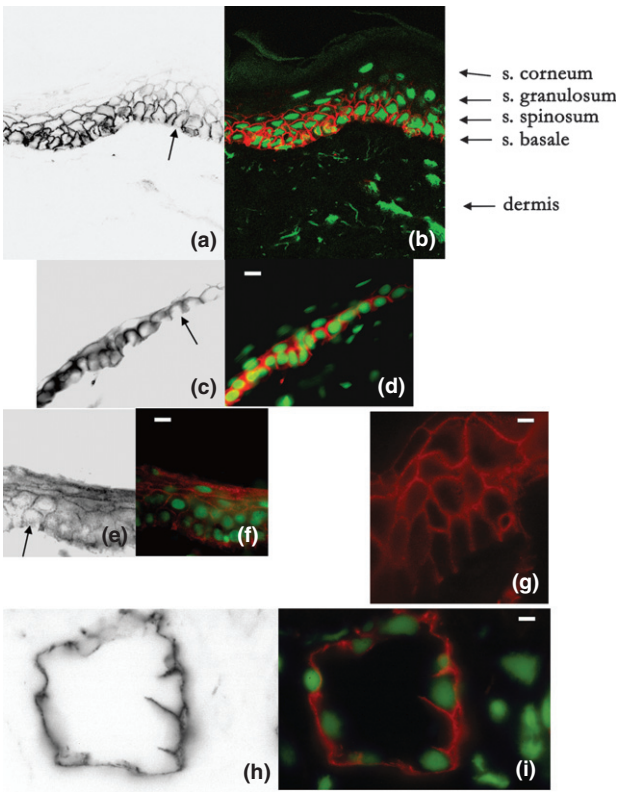

Figure 2. Immunohistochemical detection of Na,K-ATPase and non-gastric H,K-ATPase in mammalian epidermis, and Na,K-ATPase in Xenopus skin. a, b, c, d – labelling with anti-α1 monoclonal antibody αF6; e, f – labelling with anti-αng monoclonal antibody B11; g, h, i – labelling with anti-Na,K-ATPase α-subunit rabbit polyclonal antibodies; a, b, e, f – human skin; c, d – rat skin; g, h, i – Xenopus skin (g – epidermis; h, i – glandular ducts); a, b – confocal images; c–i – wide-field images. a, c, e, h – inverted black and white images of Alexa Fluor-594 fluorescence; b, d, i – merged images with green fluorescence representing nuclei stained with SYBR Green. Bars, 10 μm. In mammalian skin, both universal anti-Na,K-ATPase α polyclonal antibodies and α1 monoclonal antibody show virtually identical labelling patterns (not shown).

in epidermis over total newborn skin. It should be noted that adult skin has a higher level of FXYD4, whereas newborn skin has higher levels of FXYD6, ATP1A1 and ATP1B4 (Fig. 1 and Fig. S1).

A monoclonal antibody against Na,K-ATPase α1 isoform produces bright labelling of plasma membranes in both rat and human epidermal cells (Fig. 2a–d). In images 2a and 2b, where epidermis is stratified, it is clearly seen that Na,K-ATPase is highly abundant in all cells of *stratum basale*. *Stratum spinosum* is labelled to a lower extent, *stratum granulosum* (the most outward layer of live cells) is almost unlabelled and *stratum corneum* (dead cornified cells) is not labelled above background. Therefore, Na,K-ATPase is gradually lost in the process of keratinization. Similarly, Na,K-ATPase is expressed in basal cells of cultured differentiated keratinocytes (14). Na,K-ATPase is absent from basal membrane of the *stratum basale* (Fig. 2a, c; arrows). This is especially evident in case of poorly stratified rat scrotal epidermis (Fig. 2c). Hence, Na,K-ATPase in cells of *stratum basale* displays lateroapical localization.

A monoclonal antibody against the α-subunit of human non-gastric H,K-ATPase shows a different labelling pattern (Fig. 2e, f). All layers of live cells are positive with higher intensity in *stratum granulosum.* Interestingly, not only plasma membranes are labelled but some diffuse labelling is also present that may reflect retention of non-gastric H,K-ATPase in intracellular stores.

Polyclonal antibodies against Na,K-ATPase produce bright labelling of plasma membranes of *Xenopus laevis* epidermal cells (Fig. 2g, Fig. S5). Epidermis is labelled much stronger than cells in underlying skin layers. *Stratum corneum* is not labelled above background. However, the Na,K-ATPase is not lost from lower to upper layers so sharply as in mammals, thereby reflecting the morphological differences in the stratification patterns between terrestrial mammals and mostly aquatic Amphibia. Na,K-ATPase in cells of *stratum basale* has lateroapical localization (Fig. 2g). In contrast, Na,K-ATPase in epithelial cells of the glandular ducts shows strict basolateral intracellular polarization (Fig. 2h, i). It also should be noted that the ductal Na,K-ATPase labelling is much more intense than in the surface-exposed epidermis. The basolateral Na,K-ATPase in Xenopus ductal epithelium is in line with reports on basolateral localization of Na,K-ATPase in mammalian sweat glands (15,16). This fact illustrates that patterns of Na,K-ATPase localization in the skin are conserved from amphibians to mammals.

Conclusions

Postnatal skin maturation is associated with an increase in FXYD4 expression and a decrease of Na,K-ATPase α1 subunit, FXYD6 and ATP1B4. Na,K-ATPase of rat epidermis is represented predominantly by α1 and β3; keratinization is associated with loss of Na,K-ATPase α-subunit and an enrichment of αng. Na,K-ATPase has conserved lateroapical polarization in epidermis, which may be coupled to the NHE exchanger and thus may be important for surface acidification of the epidermis.

Acknowledgements

We are grateful to Drs. A. Quaroni and J. Kyte for antibodies. We thank Drs. I. de la Serna and A. Beavis for valuable comments on the manuscript. This work was supported by RFBR (11-04-12112 and 13-04-01413) and MCB RAS.

Author contributions

N.B.P. and N.N.M. planned experiments, N.B.P. and T.V.K. performed experiments, N.B.P. and M.I.S analysed and interpreted the data, N.B.P., T.V.K. and M.I.S. prepared figures, and N.B.P. and N.N.M. wrote the manuscript.

Conflict of interests

The authors have declared no conflicting interests.

References

1 Sakuntabhai A, Ruiz-Perez V, Carter S *et al.* Nat Genet 1999: **21**: 252–253.
2 Hu Z, Bonifas J M, Beech J *et al.* Nat Genet 2000: **24**: 61–65.
3 Grishin A V, Sverdlov V E, Kostina M B *et al.* FEBS Lett 1994: **349**: 144–150.
4 Bchetnia M, Tremblay M L, Leclerc G *et al.* Hum Genet 2012: **131**: 393–406.
5 Suárez-Fariñas M, Li K, Fuentes-Duculan J *et al.* J Invest Dermatol 2012: **132**: 2552–2564.
6 Geering K. 2005: J Bioenerg Biomembr **37**: 387–392.1.
7 Koefoed-Johnsen V, Ussing H H. Acta Physiol Scand 1958: **42**: 298–308.
8 Hachem J P, Behne M, Aronchik I *et al.* J Invest Dermatol 2005: **125**: 790–797.
9 Pestov N B, Korneenko T V, Shakhparonov M I *et al.* Am J Physiol Cell Physiol 2006: **291**: C366–C374.
10 Riemer A B, Keskin D B, Reinherz E L. Exp Dermatol 2012: **21**: 625–629.
11 Jung M, Lee S, Park H Y *et al.* Exp Dermatol 2011: **20**: 314–319.
12 Tsutsumi M, Goto M, Denda S *et al.* Exp Dermatol 2011: **20**: 464–467.
13 Kone B C, Higham S C. J Biol Chem 1998: **273**: 2543–2552.
14 Yuki T, Haratake A, Koishikawa H *et al.* Exp Dermatol 2007: **16**: 324–330.
15 Quinton P M, Tormey J M. J Membr Biol 1976: **29**: 383–399.
16 Saga K. Prog Histochem Cytochem 2002: **37**: 323–386.

Supporting Information

Additional Supporting Information may be found in the online version of this article:

Data S1. Materials and methods.
Data S2. Supplemental results.
Data S3. Supplemental references.
Table S1. Oligonucleotide primers for real-time RT-PCR.
Figure S1. Postnatal regulation of some X,K-ATPase genes in rat skin. Presented are real-time RT-PCR ΔC_t values of 7 genes with PPIA (cyclophilin A) as the housekeeping gene ($\Delta C_t = C_t^{\text{gene of interest}} - G_t^{\text{PPIA}}$). Mean ΔC_t values shown as thin horizontal lines.
Figure S2. Detection of Na,K-ATPase β1 subunit in rat skin. Labeling with anti-β1 monoclonal antibody IEC 1/48; Left panel - inverted black and white images of Alexa Fluor-594 fluorescence; Right panel - merged image with green fluorescence representing nuclei stained with SYBR Green. Bar, 10 μm.
Figure S3. Detection of several X,K-ATPase subunit proteins by immunoblotting. **A** – β3 isoform detection with guinea pig anti-rat β3 polyclonal antibodies (Right panel – negative control). **B** – total Na,K-ATPase detection with pan-specific antibodies against KETYY C-terminal peptide (Left panel – negative control). **C** – α2 Na,K-ATPase isoform using a monoclonal antibody (Peng et al) (Left panel – negative control). Rather faint α2 bands (weaker than nonspecific ones) can be seen with very long exposure time (results not shown). 1,2,3,4 – membrane-enriched rat skin fractions: 1 – 0.5 day, 2 - 15 day, 3 – 50 day, 4 – 1 year old, 5 – rat brain membranes.
Figure S4. Mitochondria-rich cells in Xenopus epidermis. Inverted black and white image of Alexa Fluor-594 fluorescence. Detection of mitochondria-rich cells with monoclonal antibody 4F6 against nicotinamide nucleotide transhydrogenase. Contrast and brightness was adjusted so that the revealed nonspecific binding allows better visualization of the epidermal structure.
Figure S5. Na.K-ATPase in Xenopus epidermis. Labeling with anti-Na,K-ATPase pan-specific polyclonal antibodies (red fluorescence). Stratum corneum is visualized by its green autofluorescence.
Figure S6. Na,K-ATPase in rat epidermis. Labeling with anti-Na,K-ATPase pan-specific polyclonal antibodies (red fluorescence). Blue fluorescence – DAPI-labeled nuclei.